DOI: https://doi.org/10.46354/i3m.2019.imaaca.001

A COMBINED BOND GRAPH-BASED – DATA-BASED APPROACH TO FAILURE PROGNOSIS

W. Borutzky

Bonn-Rhein-Sieg University of Applied Sciences, St. Augustin, Germany

ABSTRACT

Given known control inputs and real sensor outputs or simulated measurements, the paper shows that numerical values of unknown parameter degradation functions can be obtained by evaluating equations derived from a bicausal diagnostic bond graph that are not analytical redundancy relations. Inspection of causal paths beforehand enables to decide whether potential parametric faults can be isolated with a number of sensors in given locations. The proposed approach can be applied in the case of multiple isolated simultaneous parametric faults. Numerical values of degradation functions can be computed concurrently to the constant monitoring of a system and the measurement of signals. Repeatedly projecting the time evolution of a degradation function into the future based on values in a sliding time window enable to obtain a sequence of remaining useful life estimates. The novel proposed combined bond graph-model-based, data-based approach is verified by an offline simulation study of a typical power electronic circuit.

Keywords: Sensor placement and fault isolation, a priori unknown parameter degradation functions, bicausal Bond Graphs, failure prognosis, remaining useful life.

1. INTRODUCTION

Nowadays, more and more mechatronic engineering systems are equipped with sensors and embedded systems so that they can process measured information, detect and isolate emerging faults and may reconfigure their control themselves. Beyond safety and reliability of safety critical engineering systems and processes, these capabilities are of significant importance for supervision, automation and condition based maintenance of industrial processes, for an intelligent communication and cooperation of networked robots, or for all kinds of emerging autonomous intelligent operating mobile systems such as unmanned aerial vehicles, or for cyber physical systems.

Accordingly, fault detection and isolation (FDI) has been a major subject in research and in various application fields. Approaches to FDI are commonly based on either measured data or on models In addition, recently also a combination of model-based and data-based approaches has been proposed Jha (2015).

With regard to fault isolation a question is how many sensors are to be placed in which locations in order to isolate a maximum of potentially faulty system components. This is still a subject of ongoing research. Various approaches to the sensor placement problem based on bipartite graphs Frisk et al (2009), on digraphs Alem and Benazzouz (2013), or on bond graphs Djeziri et al (2009); Benmoussa et al (2014); Chi and Wang (2015); Borutzky (2018b) have been reported in the literature.

Once, a fault has been diagnosed, another question is how long a system may safely continue its operation despite the presence of an incipient fault before the increasing affect of the fault on the dynamic system behaviour may lead to a component or even a system failure. Clearly, constant monitoring of the health of a system and a repeated prediction of the remaining useful life (RUL), i.e. failure prognosis is of technical and economical importance. Online failure prognosis is also a subject of ongoing research.

To anticipate the RUL as of the current time instant, it is necessary to know the degradation behaviour of a fault over time. To that end one may try to develop a model of the degradation process starting from physical principles. Difficulties, however, may be that the degradation process is not fully understood or that not all needed parameters of a degradation model can be determined.

Other options may be to obtain a degradation model from offline accelerated life tests Escobar and Meeker (2006) and to use the results in online health monitoring for the prediction of the RUL Medjaher, K. and Zerhouni, N. (2013), or to assume that a potential degradation function candidate is a member of a certain class of functions and to adapt the unknown parameters of the function by curve fitting. As measured signals carry noise, a RUL has to be considered a stochastic quantity Jha (2015).

Moreover, for systems operating in various modes, the degradation behaviour may change from mode to mode making it necessary to change to another class of potential degradation functions (Borutzky, 2016, Chap. 6).

In order to avoid the disadvantages pertaining to the development of a degradation model from physical principles and as well to curve fitting based on measurements, Borutzky recently proposed to estimate the numerical values of an unknown degradation function from the time series of analytical redundancy relations (ARRs) derived from a diagnostic bond graph (DBG) Borutzky (2018a). The approach uses a first stage and a second stage DBG. An evaluation of ARRs obtained from a DBG with nominal parameters and inputs from the real faulty system or a model of it must result in some residuals significantly different from zero. A second stage DBG accounts for the

ISBN 978-88-85741-31-7; Bruzzone, Dauphin-Tanguy and Junco Eds

unknown degradation function of a component parameter. Accordingly, ARRs derived from the second stage DBG must be close to zero. The use of ARR residuals from the first stage DBG in the ARRs of the second stage DBG leads to an equation that determines the unknown degradation function.

A different approach recently reported in Prakash et al (2018) also evaluates ARRs but obtains degradation data by repeated updating a faulty parameter. Once a faulty parameter is identified, its value replaces the current parameter value which means that the model is adapted to the current faulty situation. Accordingly, an evaluation of the ARR sensitive to fault under consideration should provide a residual close to zero. However, as the magnitude of the fault progressively increases with time, a repeated evaluation of the ARR after some time step will result in new residual. Identification of the new faulty parameter value gives another estimated value of the unknown degradation function.

This paper continues the work in Borutzky (2018a) by showing that a more direct approach based on a *single bicausal* DBG can provide the same results and does not need ARRs. Determining the numerical values of a degradation function means to evaluate the magnitude of a fault for each time instant. Clearly, to that end, the faulty component must have been isolated. Therefore, in the following, first, the placement of sensors aiming at a fault isolation is addressed. It is assumed that the observed faulty system behaviour is due to a component parameter that has become time-varying as of some time instant.

Given known system inputs and either measurements from a real system or simulated measurements, the objective of the single bicausal DBG based approach proposed in this paper is to numerically determine an unknown parameter degradation function by estimating the numerical values of a faulty parameter for each time instant that can be used in data-based failure prognosis. As in Prakash et al (2018), the numerical values of an unknown degradation function are determined over a sliding time window of fixed size. For each time window, the data-based part of the approach identifies a mathematical function and projects it into the future to obtain an estimate of the current RUL. As a result, a sequence of RUL estimates is obtained with values that tend to zero as the considered faulty component reaches its end of life (EOL).

The approach proposed in this paper is explained by means of a typical power electronic circuit. Results are verified by an offline simulation study. The presentation continues by addressing the estimation of the RUL and concludes with a discussion of some aspects that may be subject of further considerations.

2. SENSOR PLACEMENT AND FAULT ISOLATION

In Borutzky (2018b), Borutzky proposes a graphical approach to the isolation of parametric component faults that aims at avoiding the limitations of an inspection of

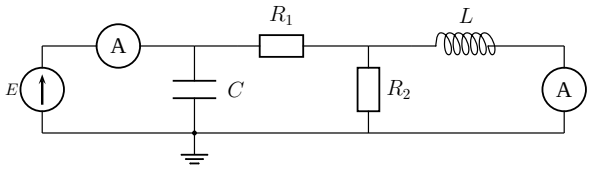

Figure 1: Circuit schematic

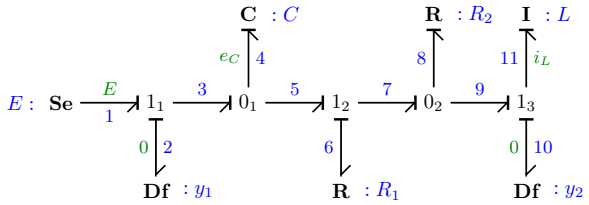

Figure 2: BG of the circuit in Fig. 1

a structural fault signature matrix (FSM) and the computational costs of numerical methods. Briefly, the idea is to start from a DBG of a system with given sensors, consider causal paths and to add repeatedly detectors to the DBG so that a maximum of disjoint causal paths from detectors to possibly faulty elements is obtained. If are there causal paths from different detectors to a potentially faulty element, the set of these non-disjoint causal paths must be unique. A parameter fault in these elements can be isolated as can be verified by a FSM. As it is known, a structural FSM can be directly obtained from a DBG by following causal paths. As there may be technical limitations as to where sensors can be placed, a detector may not be attached to some junctions in the DBG. Moreover, some parameter faults cannot be isolated without inserting additional junctions and attaching a detector to it. For instance, a flow sensor is not enough to isolate the parameters of electrical elements connected in series.

The issue of fault isolation and sensor placement is illustrated by means of a small electrical circuit that has also been considered by Frisk et. al. in Frisk et al (2009).

The circuit schematic with two non-faulty flow sensors in Fig. 1 is easily converted into the BG in Fig. 2. The model is of order one as the capacitor must take derivative causality. As there is a causal path from the inductor I : L to the detector Df : y_2 and since no storage element remains in integral causality when preferred derivative causality is assigned, the circuit is completely state observable with the sensor Df : y_2. However, as to FDI, even if the voltage source Se : E and the flow sensor Df : y_2 are assumed to be faultless, one sensor is certainly not enough to isolate more than one parametric fault. That is, additional real or virtual sensors are needed. For the two output variables, y_1, y_2, the following two equations can be derived from the BG in Fig. 2.

$$y_1 = -\frac{R_2}{R_1+R_2} i_L + \frac{1}{R_1+R_2} E + C\frac{d}{dt}E \quad (1)$$

$$y_2 = i_L \quad (2)$$

ISBN 978-88-85741-31-7; Bruzzone, Dauphin-Tanguy and Junco Eds

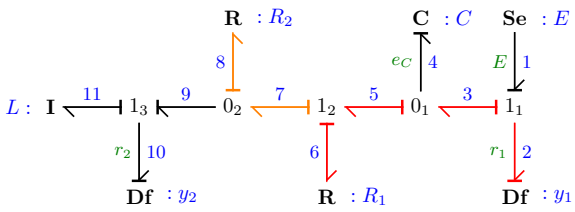

Figure 3: DBG of the circuit in Fig. 1

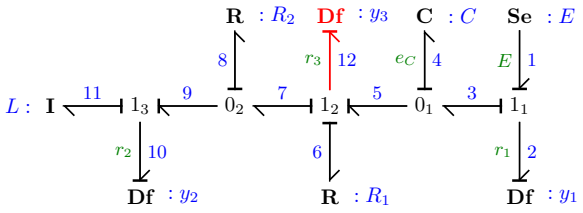

Figure 4: DBG of the circuit in Fig. 1 with an additional flow detector Df : y_3

Table 1: Structural fault signature matrix of the circuit in Fig. 1 with two current sensors

Element	r_1'	r_2'	D_b	I_b
Se : E	1	0	1	0
C : C	1	1	1	0
I : L	0	1	1	(1)
R : R_1	1	0	1	0
R : R_2	1	1	1	0

Table 2: Structural fault signature matrix of the DBG in Fig. 3 with detectors Df : y_1, Df : y_2 and Df : y_3.

Element	r_1	r_2	r_3'	D_b	I_b
Se : E	1	0	0	1	1
C : C	1	0	1	1	1
I : L	0	1	0	1	1
R : R_1	0	0	1	1	1
R : R_2	0	1	1	1	1

Given the input E and the state variable i_L, (1) may be considered the equation of a virtual sensor that provides the output y_1. The question is, how many sensors are needed to isolate a maximum of number of potentially faulty element parameters.

Now, for FDI, the circuit schematic in Fig. 1 is transformed into the diagnostic bond graph (DBG) in Fig. 3 with detectors in inverted causality and storage elements in preferred derivative causality. As can be seen, there are two non-disjoint causal paths from detector Df : y_1 to resistors R : R_1 and R : R_2. That is, these parameters cannot be isolated. If one of the two resistors becomes faulty, the degradation of its resistance cannot be computed given the two sensors.

As there are two sensors in the circuit, two ARRs can be set up from the DBG in Fig. 3.

$$\begin{aligned} \text{ARR}_1: \quad r_1' &:= r_1 + (R_1+R_2)C\dot{r}_1 \\ &= E + (R_1+R_2)C\dot{E} - (R_1+R_2)y_1 + R_2 y_2 \quad (3) \\ \text{ARR}_1: \quad r_2' &:= r_2 - R_2 C\dot{r}_1 \\ &= R_2(y_1 - y_2) - R_2 C\dot{E} - L\dot{y}_2 \quad (4) \end{aligned}$$

Accordingly, the structural FSM in Table 1 displays which element parameters contribute to which ARR. As the entry '1' highlighted in blue in the last column of Table 1 indicates, only a potentially faulty inductor I : L can be structurally isolated given the two flow sensors.

Following the graphical procedure proposed in Borutzky (2018b), attaching an additional flow detector Df : y_3 to junction 1_2 (Fig. 4) yields disjoint causal paths from detectors to elements except the two causal paths from detectors Df : y_2 and Df : y_3 to the resistor R : R_2. They indicate that R_2 contributes to the two ARR residuals r_2, r_3 giving rise to an element fault signature that is unique. As a result, all possibly faulty elements can be isolated given these three sensors[1]. The result of this bond graph based procedure is confirmed by the structural FSM in Table 2 and is in accordance with the result obtained by the bipartite approach in Frisk et al (2009).

Depending on the structure of a DBG, attaching additional sensors to its junctions in certain places can not always increase the number of disjoint causal paths from detectors to potentially faulty elements and thus increase the number of parametric faults that can be structurally isolated. As an example, consider the DBG model of a DC motor that moves a rotational mechanical load against an external torque T displayed in Fig. 5.

With the given flow detectors Df : i_a for the armature current and Df : ω_l for the angular load velocity none of the potentially faulty parameters can be isolated. The result is only partially improved by adding a flow detector Df : ω_m to junction 1_2 for the angular velocity of the motor connected to the load by a shaft with some flexibility C : C_s. The added flow detector enforces integral causality at the C-element C : C_s so that the ARR obtained by the sum of flows at junction 1_2 must be differentiated to get rid of the initial condition of the integration. Nevertheless, only two potentially faulty parameters can be isolated as indicated in the FSM of Table 3

As the voltage supply of the motor, the resistance R_a and the inductance L_a of the armature are in series, one flow detector for the current through these elements is not enough to isolate their parameters. Additional junctions $(0_2, 0_3)$ with detectors attached to them must be inserted into the DBG as shown in Fig. 6

So far, sensors have been assumed to be faultless. If this is not the case, a faulty sensor can be modelled by a

[1] Note, as Df : y_3 entails integral causality on C : C the ARR for r_3 is differentiated with respect to time to get rid of the initial condition.

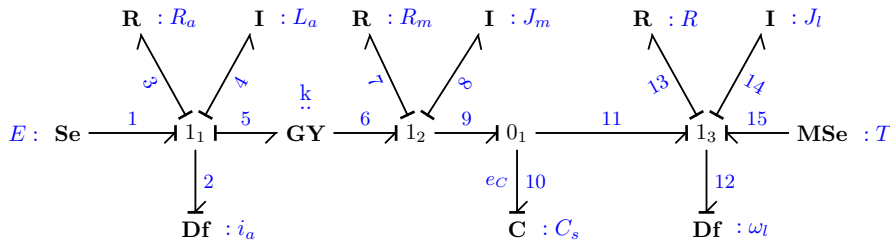

Figure 5: DBG of a DC motor drive with two flow sensors Df : i_a and Df : ω_l (Borutzky (2018b))

Table 3: FSM of the DBG in Fig. 5 with an additional flow detector Df : ω_m

Element	r_1	r_2	r_3	D_b	I_b
Se : E	1	0	0	1	0
MSe : T	0	1	0	1	0
R : R_a	1	0	0	1	0
I : L_a	1	0	0	1	0
GY : k	1	0	1	1	①
R : R_m	0	0	0	1	0
I : J_m	0	0	0	1	0
C : C_s	0	1	1	1	①
R : R	0	1	0	1	0
I : J_l	0	1	0	1	0

detector of the faultless signal and a modulated sink that provides the faulty signal component. Clearly, a faulty sensor cannot be used for detection and isolation of parametric faults of system components. Therefore, another non-faulty sensor is needed that enables to isolate the sensor fault. For illustration, consider the small passive network in Fig. 7 with a faulty sensor for the inductor current. The DBG in Fig. 8 reflects that the sensor measures a faulty inductor current $\tilde{i}_L = i_L + \Delta i_L$. As can be seen, there is a direct causal path p_1 from the additional detector De : u_s to the modulated sink MSf : Δi_L and another path p_2 to the inductor I : L which means that the sensor fault Δi_L affects ARR residuals r_2 and r_3. Moreover, there is an indirect causal path p_3 from detector Df : y_1 via R : R_2 to the sink MSf : Δi_L. That is, Δi_L also contributes to ARR_1, hence, all three ARRs.

Moreover, there are the following direct causal paths

p_4: Df : $y_1 \to 1_1 \to Se : E$
p_5: Df : $y_1 \to 1_1 \to 0_1 \to R : R_2$
p_6: Df : $i_L \to 0_2 \to 1_2 \to 0_1 \to R : R_2$

The last two paths indicate that R_2 contributes to residuals r_1 and r_2. As a result, the sensor fault Δi_L can be structurally isolated. This can be verified by reading out the following ARRs from the DBG in Fig. 8 and by capturing their structural parameter dependencies in the FSM

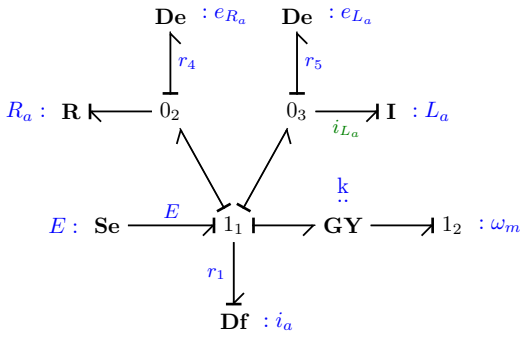

Figure 6: DBG fragment with inserted junctions 0_2 and 0_3 and attached effort detectors for further isolation of element parameters

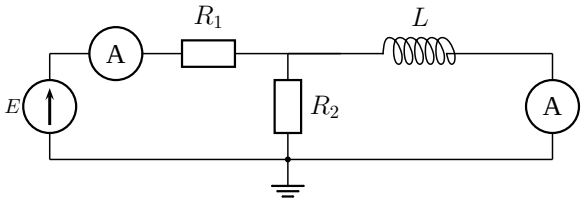

Figure 7: Circuit with a faulty sensor for the inductor current

in Table 4.

$$\mathrm{ARR}_1: \quad r_1 = E - R_2(y_1 - (i_L + \Delta i_L)) - R_1 y_1 \tag{5}$$
$$\mathrm{ARR}_2: \quad r_2 = R_2(y_1 - (i_L + \Delta i_L)) - u_s \tag{6}$$
$$\mathrm{ARR}_3: \quad \dot{r}_3 = \frac{d}{dt} i_L + \frac{d}{dt}\Delta i_L - \frac{1}{L} u_s \tag{7}$$

Potentially faulty elements Se : E and R : R_1 cannot be isolated. There are direct causal paths to these elements from detector Df : y_1 but no causal paths from the other detectors.

3. NUMERICAL DETERMINATION OF UNKNOWN DEGRADATION FUNCTIONS

Parametric degradation means that performance degradation of an engineering system is due to the fact that some of its parameters increasingly deviate from their nominal values with time following a function of which an exact analytical expression is mostly unknown.

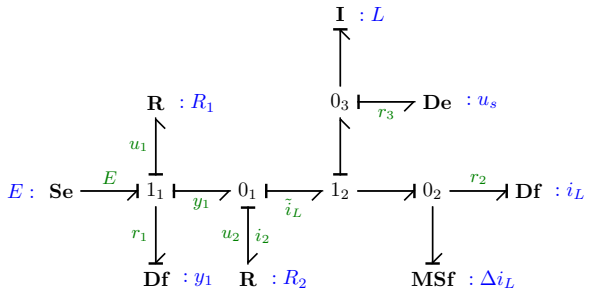

Figure 8: DBG of the circuit in Fig. 7

Table 4: Fault signature matrix of the DBG in Fig. 8

Element	r_1	r_2	r_3'	D_b	I_b
Se : E	1	0	0	1	0
R : R_1	1	0	0	1	0
R : R_2	1	1	0	1	1
I : L	0	0	1	1	1
MSf : Δi_L	1	1	1	1	1

One way to approximate a degradation trend, may be to develop a model based on physical laws. Problems, however, may be that the physics of a degradation process are not well understood or that values for some parameters of a degradation model are not available.

Alternatively, one may select a member of an appropriate class of potential degradation functions in analytical form and adapt its unknown parameters by curve fitting.

Another option may be to consider the determination of numerical values of an unknown degradation function as a parameter estimation problem.

To that end, a bicausal bond graph is used in this paper. Bicausal BGs were introduced by Gawthrop Gawthrop (1995) They extend the concept of computational causality by allowing that both co-variables, effort and flow of a bond may be inputs into a power port of an element. Accordingly, they may be used for parameter estimation and thus can be used for setting up an equation that determines the degradation function of a faulty element parameter $\Theta(t)$ at time instant t. Bicausal bond graphs have been used for FDI, e.g. in Samantaray and Ghoshal (2008). However, to the best of the author's knowledge, they haven't been used in online failure prognosis for the determination of numerical values of an unknown degradation function as proposed in this article. The approach is explained by means of a small power electronic circuit and verified by an offline simulation study in the next section.

3.1 A power electronic example

Consider the circuit schematic of a boost converter in Fig.9. It is assumed that the converter used, e.g. in power generation plants, operates in continuous conduction mode (CCM) with a sensor for the inductor current i_L and a sensor of the output voltage V. A fault in this system component may lead to a failure in a power distribution system or to a degradation of its performance.

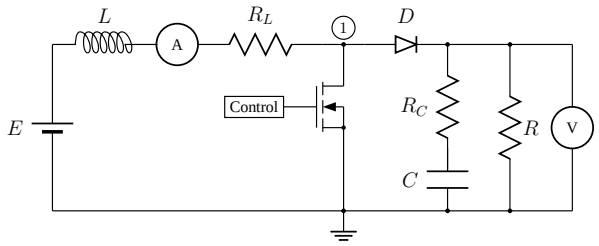

Figure 9: Circuit schematic of a boost converter (Borutzky (2018a))

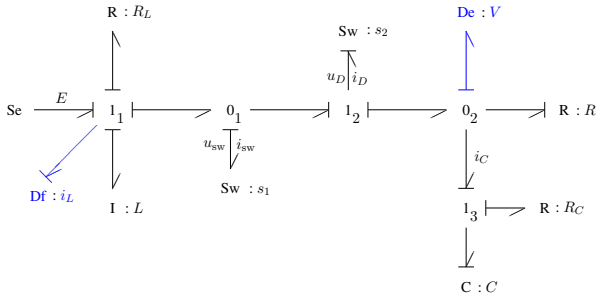

Figure 10: DBG of the boost converter in Fig. 9 (Borutzky (2018a))

If the MOSFET transistor and the diode are modelled as two conversely commutating ideal switches Sw : s_i, $i = 1,2$, then the circuit immediately transforms into the DBG in Fig. 10. If the small equivalent series resistance, R_C, of the capacitor is neglected and if variables are averaged over the switching period, then the circuit may be presented by the DBG in Fig. 11, in which d denotes the duty ratio. From the DBG in Fig. 11, the following two ARRs are easily derived.

$$\text{ARR}_1 : r_1 = E - R_L - L\frac{d}{dt}\tilde{i}_L - (1-d)\tilde{V} \qquad (8)$$

$$\text{ARR}_2 : r_2 = (1-d)\tilde{i}_L - C\frac{d}{dt}\tilde{V} - \frac{1}{R}\tilde{V} \qquad (9)$$

Their structural dependencies from element parameters is represented by the FSM in Table 5. As can be seen, all parametric faults can be detected by means of the two sensors but none can be isolated apart from the faulty duty ratio d.

In the following, two general cases are considered illustrated by means of the small boost converter circuit. Firstly, it is assumed that the parameter of a resistive element is degrading with time. The other scenario is that the parameter of a storage elements progressively deviates from its nominal value. For both cases it is shown how the values of the respective unknown degradation function can be estimated by means of known inputs and measured values or simulated measurements.

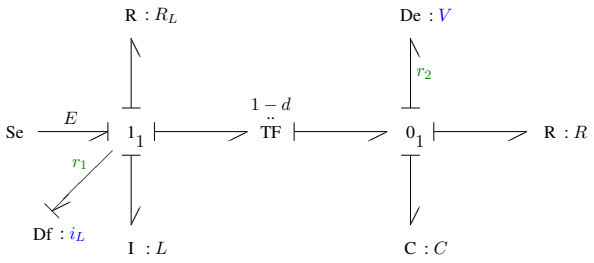

Figure 11: Averaged DBG of the boost converter in Fig. 9

Table 5: Fault signature matrix of the DBG in Fig. 11

Element	r_1	r_2	D_b	I_b
Se : E	1	0	1	0
R : R_L	1	0	1	0
I : L	1	0	1	0
TF : d	1	1	1	(1)
C : C	0	1	1	0
R : R	0	1	1	0

3.2 Degradation function of a resistor

Assume that by means of additional sensors the cause of an abnormal dynamic behaviour has been isolated and is attributed to a resistance R that is increasingly deviating from its nominal value R_n with time, i.e. $R(t) = R_n + \Phi_R(t)$. Given monitored measurements, the task is to determine the time-varying resistance $R(t)$. Accordingly, the bond attached to the port of the R-element is replaced by a bicausal bond as depicted in Fig. 12. As can be seen from the bicausal DBG in Fig. 12, there is a causal path from the flow detector Df : $\tilde{i}_L$ and another one from the effort detector De : $\tilde{V}$ to the power port of the R-element. That is, both port variables are determined by real measurements or simulated data provided by sensors into the DBG model so that the time evolution of the possibly nonlinear resistance $R(t) = R_n(t) + \Phi_R(t)$, i.e. numerical values of the degradation function $\Phi_R(t)$ can be computed. From the bicausal DBG, one obtains

$$\begin{aligned}\tilde{V} &= R(t)[(1-d)\tilde{i}_L - C_n\dot{\tilde{V}}] = [R_n + \Phi_R][(1-d)\tilde{i}_L - C_n\dot{\tilde{V}}] \\ &= R_n[(1-d)\tilde{i}_L - C_n\dot{\tilde{V}}] + \Phi_R[(1-d)\tilde{i}_L - C_n\dot{\tilde{V}}] \qquad (10)\end{aligned}$$

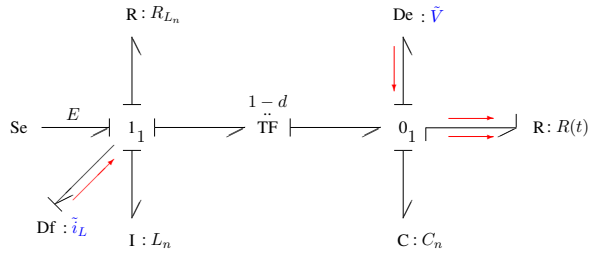

Figure 12: Averaged bicausal DBG of the boost converter

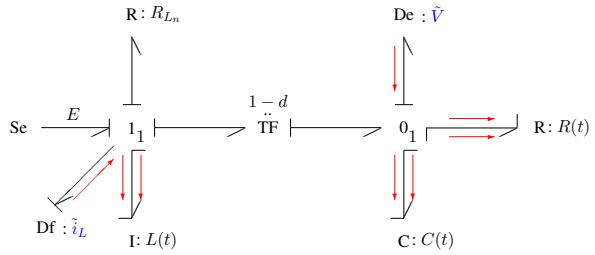

Figure 13: Averaged bicausal DBG of the boost converter

and as a result an implicit algebraic equation for the unknown degradation function $\Phi_R(t)$.

$$\Phi_R(t)[(1-d)\tilde{i}_L - C_n\dot{\tilde{V}}] = -R_n \underbrace{[(1-d)\tilde{i}_L - C_n\dot{\tilde{V}} - \frac{\tilde{V}}{R_n}]}_{=: r_2^1} \qquad (11)$$

or

$$(\tilde{V} + R_n r_2^1)\Phi_R(t) = -R_n^2 r_2^1 \qquad (12)$$

Equation (12) is identical to (21) in Borutzky (2018a), in which r_2^1 denotes an ARR residual derived from the DBG of the first stage.

3.3 Degradation function of a storage element

In the bicausal DBG of Fig. 13, the bond attached to the power port of the C-element has also been turned into a bicausal bond. As a result, there are causal paths from the two detectors to the C-port so that the numerical values of a decaying capacitance $C(t)$ could be determined. However, these causal paths are not disjoint from the ones to the R-port so that it cannot be decided whether an abnormal dynamic system behaviour is caused by a degradation of the resistance R or of the capacitance C which is also expressed by the FSM in Table 5. This is not surprising, because both elements are in parallel, the voltage drop across both elements is the same. As addressed in Borutzky (2018b), another junction with an additional detector attached is to be inserted for isolation if both elements are faulty. Therefore, the following case assumes that only the capacitance, which may be nonlinear, follows an unknown degradation function, i.e. $C(t) = C_n(t) + \Phi_C(t)$. Observing the causal paths from the detectors to the C-element, the following implicit differential equation for the degradation function $\Phi_C(t)$ can be obtained from the DBG in Fig. 13.

$$\frac{d}{dt}(\Phi_C\tilde{V}) = \underbrace{(1-d)\tilde{i}_L - \frac{\tilde{V}}{R_n} - \frac{d}{dt}(C_n\tilde{V})}_{r_2^1} \qquad (13)$$

or

$$\Phi_C(t)\tilde{V}(t) = \int_{t_{f_2}}^{t} r_2^1(\tau)d\tau + \Phi_C(t_{f_2})\tilde{V}(t_{f_2}) \qquad (14)$$

where t_{f_2} denotes the time instant when the incipient fault exceeds an (adaptive) threshold and thus is detected. That is, $\Phi_C(t) \neq 0$ for $t > t_{f_2}$. Below that threshold the value of the capacitance may vary. However, a robust fault detection neglects small deviations from nominal parameter values in order to avoid false alarms.

Equation (14) equals the result (29) in Borutzky (2018a) obtained by an approach with two diagnostic bond graphs.

Finally, as can be seen from the bicausal DBG in Fig. 13, there are another two causal paths from the detectors to the inductor with a faulty inductance $L(t) = L_n(t) + \Phi_L(t)$. The causal path from the voltage detector to the inductor is not disjoint from the causal path to the resistor R : R and the one to the capacitor. That is, these parametric faults cannot be isolated in accordance to the FSM in Table 5. If it is only the inductor that has become faulty as of a time instant t_{f_1}, then similar to the computation of $\Phi_C(t)$ above, one obtains for the unknown degradation function $\Phi_L(t)$ from the bicausal DBG

$$\frac{d}{dt}(\Phi_L \tilde{i}_L) = \underbrace{E - R_{L_n}\tilde{i}_L - \frac{d}{dt}(L_n \tilde{i}_L) - (1-d)\tilde{V}}_{=: r_1^1} \quad (15)$$

or

$$\Phi_L(t)\tilde{i}_L(t) = \int_{t_{f_1}}^{t} r_1^1(\tau)d\tau + \Phi_L(t_{f_1})\tilde{i}_L(t_{f_1}) \quad (16)$$

where r_1^1 equals a first stage DBG ARR residual obtained by the two DBGs approach in Borutzky (2018a). The integration in (14), (16) may be performed by means of the trapezoidal rule.

4. OFFLINE SIMULATION STUDY

In the following, the above numerical determination of a capacitance degradation shall be verified in an offline simulation. That is, real measurements are replaced by simulated ones obtained from a BG model of the faulty circuit. Capacitor leakage is a typical fault. In Kulkarni et al (2010), it is reported that electrolytic capacitors in power electronic systems have a higher failure rate than other system components. In this study, it is assumed that the decay of the capacitance is exponentially with time according to the function

$$C(t) = \begin{cases} C_n & t < t_0 \\ \frac{1}{5}C_n + \frac{4}{5}C_n e^{-\lambda(t-t_0)} & t \geq t_0 \end{cases} \quad (17)$$

That is, as of time instant t_0 the capacitance reduces exponentially with $t \to \infty$ to one fifth of its nominal value C_n.

The objective of the simulation is to recover this degradation from available 'measured' data $\tilde{i}_L$ and $\tilde{V}$ provided by a model with variables averaged over the switching period. Although averaging results in some smoothing, measurement noise is taken into account by adding 1% Gaussian noise to the output signals of the BG model. In

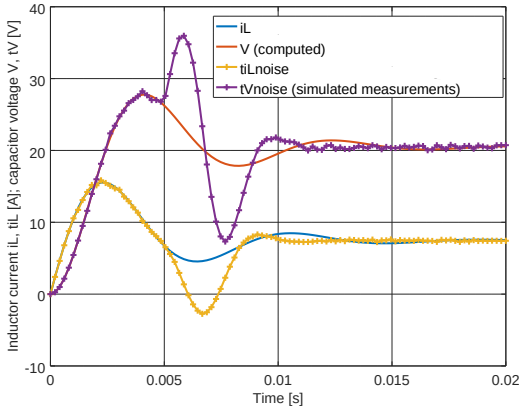

Figure 14: Effect of the capacitor degradation as of $t_f = 0.005s$ on the inductor current $\tilde{i}_L$ and the capacitor voltage $\tilde{V}$

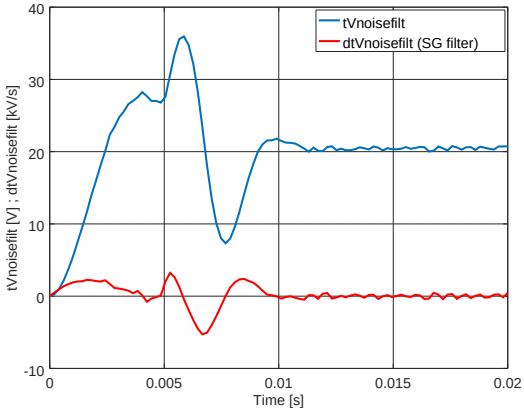

Figure 15: Filtered noisy capacitor voltage tVnoisefilt and its derivative dtVnoisefilt

a bicausal DBG, measurement uncertainties can be represented by modulated sinks (cf. Fig. 8).

The simulation performed by the free software GNU Octave 4.4.1 uses the parameters given in Table 6. The effect of the capacitance degradation on the inductor current $\tilde{i}_L$ and the capacitor voltage $\tilde{V}$ is displayed in Fig. 14 in which the tilde is substituted by the letter t prefixing the variable name. Simulated noisy measurements are obtained by means of the Octave function `randn()`.

```
tV = tV + 0.01*tV .* randn(linspace(tV)) (18)
```

The noisy signals have been smoothed by a Savitzky-Golay filter Savitzky, A. and Golay, M.J.E. (1964) (Octave function `sgolayfilt()`). In (11), the derivative of the simulated measurement $\tilde{V}$ is needed. Differentiation and smoothing has also been carried out by a Savitzky-Golay filter. The result is displayed in Fig. 15.

Fig. 16 finally displays the recovered decay of the capacitance $rC(t)$.

As can be seen, the time evolution of the recovered capacitance $rC(t)$ is sufficiently close to the decay of the capacitance $C(t)$ deliberately introduced into the be-

Table 6: Parameters of the averaged DBG model in Fig. 11

Parameter	Value	Units	Meaning
E	12.0	V	Voltage supply
L	1.0	mH	Inductance
R_{L_n}	0.1	Ω	Resistance of the coil
C_n	500	μF	Nominal capacitance
R_n	5.0	Ω	Nominal load resistance
T_s	10^{-3}	s	Switching time period
d	0.45	–	Duty ratio
t_f	0.005	s	Capacitance starts decline
λ	500	s^{-1}	Rate of decline

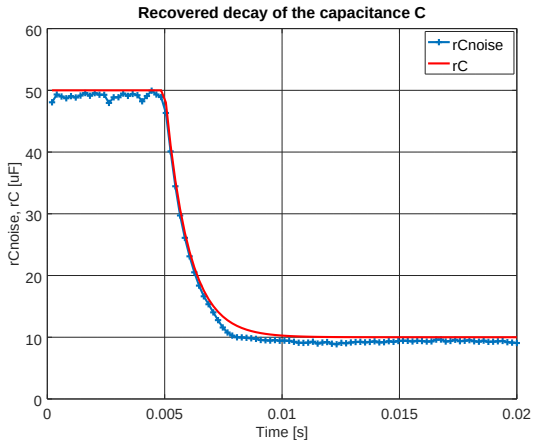

Figure 16: Recovered capacitance rC(t), rCnoise(t)

havioural model of the circuit.

5. REMAINING USEFUL LIFE ESTIMATION

As explained and illustrated in Section 3, equations for unknown parameter degradation functions for resistive as well as storage elements can be directly derived from a bicausal diagnostic bond graph by following causal paths from sources and detectors in inverted causality to the port of a faulty element. That is, inputs to these equations are only known control inputs and measurements. Numerical values of a parameter degradation function can be computed online concurrently to the monitoring of the health of a real system and the constant measurement of signals. As soon as n measured values of each needed signal are available and stored in a buffer, the time evolution of a faulty parameter $\Theta(t)$ can be approximated up to a time instant t and can be projected into the future to see when it would intersect with a failure threshold.

5.1 Data-driven failure prognosis

Once computed numerical values of an unknown function of the degradation of parameter Θ_i are available, they may be treated like degradation data of a feature extracted from measurement data. Direct measurement of degradation is often not possible without being invasive or destructive. The computation of a time-series of degradation data by an evaluation of equations derived from a bicausal BG can be considered the data acquisition phase.

Given n available degradation data $\Phi_\Theta(t_i^k)$, $i = 1,\ldots,n$ obtained from real measurements or simulated measurements in a sliding time window w^k that are stored in buffer of fixed size, a number of basic mathematical models, i.e linear, exponential, or power models with parameters to be determined may be tested to see which one fits best the data in current window w_k. This task of learning a mathematical model can be carried out e.g. by a commercial software such as the Matlab Predictive Toolbox The Mathworks (n.d.) and can be performed in parallel on a multiprocessor, multicore computer. As an evaluation criterion for the best fit, the root mean square error (RSME) may be used. The degradation function $\Phi_\Theta(t)$ found can then be used to determine a time point t_f^k at which the time evolution of the faulty parameter $\Theta(t)$ intersects with a given failure level threshold.

The time span from the current time t_c^k (current age of the system) to the time instant t_f^k where the time evolution of the parameter $\Theta(t)$ obtained from degradation data in the k^{th} window w^k intersects with a failure level threshold (end of life, EOL) gives an estimate of the remaining useful life RUL^k.

$$\mathrm{RUL}^k := t_f^k - t_c^k \tag{19}$$

With progressing time new degradation values of a parameter Θ_i become available while older values drop out of the buffer. For a new time window w^k, the two steps, i.e. the determination of the best fit degradation model and its extrapolation are repeated.

As time has advanced, i.e. the system has become older, that is, t_c takes a new value and the intersection with the failure level threshold gives a new time to failure value. As a result, one obtains a new value for the RUL. Repeating these steps while time is progressing results in a sequence of k RUL estimates $\mathrm{RUL}^k(\Theta_i)$ which ultimately converge to zero as a component reaches its EOL. This two step prognosis procedure consisting of a regression analysis of the degradation data in a window and an extrapolation that provides an estimate of the time to failure can be carried out simultaneously for multiple faulty components and in parallel on a multicore,

multiprocessor computer. The global system-level RUL is then the infimum of all component RULs. An advantage of a repeated identification of a mathematical model for the degradation is that in case of a hybrid model for each system mode of operation a possibly different rate of degradation can be taken into account. In systems represented by a hybrid model, degradation of a component in ON mode may stop when the component switches into OFF mode. An example may be the mass flow through an increasingly contaminated valve. As long as the valve is open, its discharge coefficient, c_d, decreases with time. Clearly, when the valve is switched off, when this system component becomes inactive, then the last value of the discharge coefficient before closure is retained, degradation is stopped as long as the valve is in OFF mode, i.e. the decline of the time evolution $c_d(t)$ becomes zero. That is, extrapolating the time evolution of the faulty parameter from the current sliding window does provide no RUL estimate. In that system mode, the system behaviour is not affected by the faulty valve and nothing can be said about the RUL.

The numerical determination of a degradation function $\Phi_\Theta(t)$ and the projection of $\Theta(t)$ into the future requires a sufficient number of degradation data in the current window w^k in order to accurately identify the parameter of a potential degradation model. The amount of available degradation data, i.e. the size of the sliding window, affects the uncertainty in the values of the degradation model parameters and has an effect on the estimation of the time to failure. Software such as Weibull++ can compute upper and lower bounds for the time to failure with a certain confidence level. In order to meet given accuracy requirements for the parameters of the degradation model to be fitted, the size of the sliding window may vary. The boundaries for the time to failure become more narrow as the sliding time window moves on, i.e. the prediction of the time to failure becomes more accurate as a faulty component approches its EOL.

In the case of the capacitance degradation considered in Section 4, fitting of degradation data in each window gives the same exponential function $C(t)$ and its intersection with a failure threshold level C_{crit} the same time to failure t_f. Let α, β, γ be the identified parameters of the exponential function $\Phi_C(t)$ fitting the degradation data in a window. Then the time to failure t_f is determined by the condition

$$C(t_f) = \alpha C_n + \beta C_n e^{-\gamma(t_f - t_0)} = C_{\text{crit}} \qquad (20)$$

Solving for t_f gives

$$t_f = t_0 - \frac{1}{\gamma}\left(-\ln\beta + ln\left(\frac{C_{\text{crit}}}{C_n} - \alpha\right)\right) \qquad (21)$$

Equation 21 indicates that the time to failure and the RUL, $\text{RUL}(C,t) := t_f - t$ depend on the fitting parameters. The true RUL is obtained for $\alpha = 1/5$, $\beta = 4/5$ and $\gamma = 500$. These parameters and $C_{\text{crit}} = 2/5$ yield $t_f = 7.777\,\text{ms}$. Fig. 17 depicts the exact RUL.

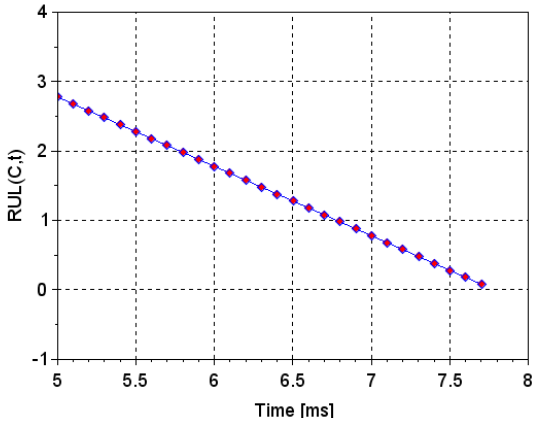

Figure 17: RUL of the decaying capacitance

5.2 Uncertainties in failure prognosis

There are some inherit uncertainties with the proposed non-residual based approach to failure prognosis.

First, the bicausal BG from which equations for unknown degradation functions are derived relies on modelling assumptions (model uncertainty).

Entries into the derived equations besides known control inputs are measurements that carry noise.

As the numerical computation of time-series degradation data is based on measurements, the parameters of a potential degradation function are to be considered random parameters for which a probability density function (pdf) has to be assumed which affects the prediction of the k^{th} time to failure t_f^k and the estimation of a RUL^k. As a result, RUL prediction does not provide a single value but a pdf. Assuming a distribution for the degradation model parameters upper and lower bounds for a RUL prediction at a time point given a required confidence level can be computed.

Prediction of the time to failure clearly depends on the failure threshold that has been set. With insufficient a priori knowledge the choice of an alarm threshold below the EOL failure threshold ensuring a safety margin is uncertain so that for a failure threshold a pdf has to be assumed. A proper choice of an alarm threshold is crucial as the intersection of an extrapolated degradation trend provides a time instant at which a decision on the action to taken must be made.

5.3 Advantages of the proposed approach

The proposed combined bond graph model-based, data-based prognosis approach has the following advantages.

The computation of numerical values of an unknown degradation function in the data acquisition phase by evaluating an equation derived from a bicausal DBG can be performed in parallel for multiple simultaneous parametric faults.

For the fitting of 'measured' degradated data pertaining to a faulty component, the parameters of various po-

tentially appropriate basic mathematical functions can be computed in parallel by means of existing software. A criterion such as the RSME can single out the best fitting function among a set of potential candidates.

The repeated identification of a best fit degradation model on the data of a sliding window enables to account for possible changes of the degradation behaviour from window to window that may be due to changes of the system mode of operation or may be caused by changes in the system's environment. Extrapolating repeatedly the time evolution of a faulty parameter from a window to the subsequent one results in a sequences of values for the time to failure and the RUL.

CONCLUSION

The paper contributes to the sensor placement problem by proposing a graphical check whether potential faulty elements can be isolated by means of a given set of sensors and how their number can be increased by adding detectors in appropriate places of a DBG model. The issue of sensor placement has been addressed because parametric fault isolation is a prerequisite for failure prognosis. Faulty sensors can be modelled as discussed in Section 2. Parametric degradation in actuators will be accounted for in future work.

Furthermore, it has been shown that by following causal paths in a bicausal DBG from detectors in inverted causality to the power port of a possibly nonlinear element with the parameter $\Theta(t)$ identified as faulty, i.e. $\Theta(t) = \Theta_n(t) + \Phi_\Theta(t)$, an equation can be established that determines the numerical values of the unknown parametric degradation function $\Phi_\Theta(t)$.

As the novel proposed computation of numerical values of unknown degradation functions is based on known input signals and on sampled values of measured signals and may require the differentiation of some signals in discrete time, sophisticated signal processing is important.

In the data-based failure prognosis part, the parameters of degradation models that best fit measured data have to be considered random with a probability density function and affects the projection into future. Uncertainties in RUL prediction have been addressed, e.g. in Sankararaman and Goebel (2013) and are considered a subject of further research.

Furthermore, there is a time delay between the occurrence and the detection of an incipient parametric fault. A parameter value deviating from its nominal value must not only touch a time dependent adaptive fault threshold but must increasingly deviate from these adaptive boundaries with time in order to be identified as a progressive fault. As a result, it takes some time until the first sliding window can be filled with degradation data.

REFERENCES

Alem S, Benazzouz D (2013) Optimal sensor placement for detection and isolation by the structural adjacency matrix. Int J of the Physical Sciences 8(6):225–230, DOI 10.5897/IJPS12.547

Benmoussa S, Ould Bouamama B, Merzouki R (2014) Bond graph approach for plant fault detection and isolation: Application to intelligent autonomous vehicle. IEEE TRANSACTIONS ON AUTOMATION SCIENCE AND ENGINEERING 11(2):585–593

Borutzky W (ed) (2016) Bond Graphs for Modelling, Control and Fault Diagnosis of Engineering Systems, 2nd edn. Springer International Publishing Switzerland, DOI 10.1007/978-3-319-47434-2

Borutzky W (2018a) Determination of a function for a degradation process by means of two diagnostic bond graphs. In: Proceedings of the 10th IFAC Symposium on Fault Detection, Supervision and Safety for Technical Processes, IFAC, Warsaw, Poland

Borutzky W (2018b) Sensor Placement on Diagnostic Bond Graphs For Maximum Structural Isolation of Parametric Faults. In: Granda J, Karnopp D (eds) Proceedings of the 13th International Conference on Bond Graph Modeling and Simulation (ICBGM'2018), SCS, Bordeaux, France, Simulation Series, vol 50(12), pp 41–49

Chi G, Wang D (2015) Sensor Placement for Fault Isolability Based on Bond Graphs. IEEE Trans on Automatic Control 60(11):3041–3046

Djeziri M, Ould Bouamama B, Merzouki R, Dauphin-Tanguy G (2009) Optimal sensor placement for fault diagnosis. In: 2009 IEEE International Conference on Mechatronics, Malaga, Spain, 2009

Escobar LA, Meeker WQ (2006) A review of accelerated test models. Statistical Science 21(4):552 – 577, DOI 10.1214/088342306000000321

Frisk E, Krysander M, Åslund J (2009) Sensor placement for fault isolation in linear differential-algebraic systems. Automatica 45:364 – 371

Gawthrop P (1995) Bicausal Bond Graphs. In: Cellier F, Granda J (eds) ICBGM'95, International Conference on Bond Graph Modeling and Simulation, SCS Publishing, Simulation Series, vol 27(1), pp 83–88

Jha M (2015) Diagnostics and prognostics of uncertain dynamical systems in a bond graph framework. PhD Thesis, École Centrale de Lille, Université Lille Nord-de-France

Kulkarni C, Biswas G, Koutsoukos X, Goebel K, Celaya J (2010) Physics of failure models for capacitor degradation in DC-DC converters. In: The Maintenance and Reliability Conference, MARCON, Knoxville, TN, U.S.A.

Medjaher, K, Zerhouni, N (2013) Hybrid Prognostic Method Applied to Mechatronic Systems. International Journal of Advanced Manufacturing Technology 69(1–4):823–834, DOI 10.1007/s00170-013-5064-0

Prakash O, Samantaray A, Bhattacharyya R, Ghoshal S (2018) Adaptive prognosis for a multi-component dynamical system of unknown degradation modes. In: Proceedings of the 10th IFAC Symposium on Fault Detection, Supervision and Safety for Technical Processes,, IFAC, Warsaw, Poland

Samantaray A, Ghoshal S (2008) Bicausal bond graphs for supervision: From fault detection and isolation to fault accommodation. Journal of the Franklin Institute 345:1–28

Sankararaman S, Goebel K (2013) Why is the Remaining Useful Life Prediction Uncertain ? In: Annual Conference of the Prognostics and Health Management Society, pp 1 – 13, open-access article

Savitzky, A, Golay, MJE (1964) Smoothing and differentiation of data by simplified least squares procedures. Analytical Chemistry 38(8):1627 – 1639

The Mathworks (n.d.) Three ways to estimate remaining useful life. White paper, https://www.mathworks.com/products/predictive-maintenance.html